Jpn Circ J 2001; **65:** 695–701

Nonfluoroscopic Endoventricular Electromechanical Three-Dimensional Mapping

— Current Status and Future Perspectives —

Glenn Van Langenhove, MD, PhD; Ken Kozuma, MD; Patrick W. Serruys, MD, PhD

Nonfluoroscopic electromechanical mapping (NOGA™, Biosense-Webster, a Johnson & Johnson Company) is a recently developed technique that enables the acquisition of on-line information on the electrical and mechanical endoventricular functioning of myocardial tissue! The rationale for this new technique is 2-fold. First, none of the currently available in-cathlab methods can distinguish viable from non-viable myocardium. Accepted techniques, such as radionuclide scintigraphy and dobutamine stress echocardiography, may not be readily available, and can not be performed in the cathlab. Second, applications such as myocardial laser revascularization or intramyocardial gene-injection may prove cumbersome when performed using echocardiography or fluoroscopy with only 2-dimensional (2-D) projections available on-line! A major pitfall of these latter techniques is indeed the inability to accurately associate the 2-D positioning with a specific endocardial site, quite apart from the high X-ray exposure for both patient and physician when using fluoroscopy? Although clinical application of on-line 3-dimensional (3-D) echocardiography and magnetic resonance imaging is underway, until recently there has not been a technique for real-time 3-D guiding of intervention tools and assessment of myocardial electromechanical functioning. Nonfluoroscopic electromechanical mapping has become the first navigation technique to accurately determine the trajectory of a tool inside the human heart, to guide the interventional device to a specific site, and to meticulously couple functional and anatomical properties!

In this overview, we shall describe the NOGA™ system components, the left ventricular mapping technique, the current experimental and clinical data available, the ongoing trials and the possible future applications of this technique.

The System

The system exists of a mapping catheter, a magnetic field emitter and a workstation. The deflectable-tip catheter (NOGA-STAR™, Biosense-Webster) contains both a location sensor just proximal to its tip and standard electrodes that allow recording of unipolar and bipolar electrical signals.

(Received June 13, 2000; revised manuscript received April 26, 2001; accepted May 2, 2001)

Department of Interventional Cardiology, Thoraxcenter Rotterdam, Academic Hospital Dijkzigt, Erasmus University, The Netherlands
Mailing address: Professor Patrick W. Serruys, Head of the Department of Interventional Cardiology, Thoraxcenter Bd 418, University Hospital Dijkzigt, Dr. Molewaterplein 40, 3015 GD Rotterdam, The Netherlands. E-mail: Serruys@card.azr.nl

The locator pad placed beneath the operating table consists of 3 radiators that generate low magnetic field energy (5×10^{-5} to 5×10^{-6} Tesla). This way, the system is provided with the information necessary to resolve the location and orientation of the catheter-sensor in 6 degrees of freedom (Fig 1). The amplitude, phase and frequency of the emitted magnetic signals recorded by the location sensor allow the computer algorhitm to solve a number of complicated algebraic equations yielding the location (x, y and z) and orientation (roll, pitch and yaw) of the sensor. The NOGA™ processing unit consists of a computer that updates the acquired information in real-time, and a Silicon Graphics work station that displays the 3-D left ventricular endocardial reconstruction (Fig 2). The operator can choose any view to work with during point acquisition, can add a second view in a separate window, and can change views at any time during the mapping procedure. As well as the electrical activation maps, maximum voltage maps (showing unipolar voltages (UPV) or bipolar voltages (BPV)), local shortening maps, and bull's eyes views, there are a variety of other features of the system that would take too long to describe here in full.

Definitions and Acronyms

Point Loop Stability Measures the maximum distance between the locations of the selected point in 2 consecutive heart cycles. Low point loop stability indicates a reproducible catheter movement trajectory.

Cycle Length (CL) Stability The difference between the length of the current cycle and the average of the last 100 cycles recorded.

Local Activation Time (LAT) Stability Measure of how stable the LAT is between cycles. Reliable points show a LAT variation of less than 3 ms.

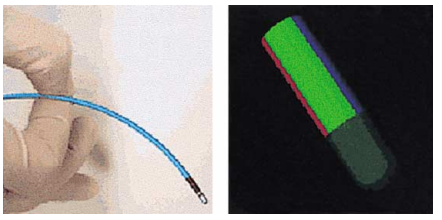

Fig 1. Close-up of the catheter tip (Left). The exact location in 3 different degrees of freedom (pitch, roll and yaw) can be appreciated throughout the procedure; at the start of the procedure, a 'calibration' must be performed in order to know the color coding of the different orientations of the catheter; for example, the green color could be the upper side of the catheter (Right).

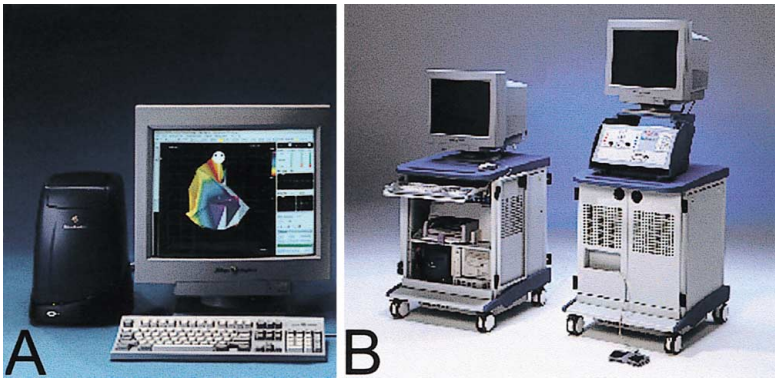

Fig 2. The system's components. (A) Work station, with the Silicon graphics computer and monitor displaying a NOGA™ map. (B) The system incorporated in a mobile cart, with the cable connecting board visible underneath the monitor.

Location Stability A measure of the variability in position of the catheter tip on the endoventricular wall during 2 consecutive cardiac cycles.

Triangle Fill Threshold By setting this value, the operator chooses the minimum triangle size for which the program will close a face on the reconstructed chamber. This feature allows the operator to determine the degree to which the system will interpolate between actual data points and will ensure that a minimal level of point density will be met at each mapped region. Usually an interpolation threshold of 30 mm between adjacent points is taken[3].

Inner Points Filtering A computer algorithm that removes points considered to be located inside the ventricular lumen (and not on the ventricular wall) or on a papillary muscle. The algorithm calculates the relative position of points as compared to at least 3 neighboring ones and is therefore able to remove these contentious points.

Local Linear Shortening (LLS) The LLS assessment is based on the assumption that in healthy myocardium any 2 points move closer to each other during contraction. Measurement of the distance between neighboring points is therefore the basis for calculation of myocardial shortening. The computer algorithm takes into account the density of points around a point 'p', and gives a negligible weight to points too close (sampling noise) and points too far (of no influence as they provide non-local information). The algorithm for regional linear shortening is calculated as follows: for any 2 points on the map, 'i' and 'j', LLS is calculated as the change in distance between these 2 points from end-diastole to end-systole, normalized for the length at end diastole:

$$LLSij = (L(ED)ij - L(ES)ij) / L(ED)ij$$

For any point 'p', LLS is calculated as a function of the LLSpj, for all points j=1 to n on the map, so that

$$LLSp = (\Sigma_{j=1..n} Wpj\,(L(ED)pj) \times LLSpj) / \Sigma_{j=1..n} Wpj,$$

where W is the weight of a certain point as a function of the distance Lij between 2 points 'i' and 'j', the average distance D around point 'p' (D is defined in the computer algorithm as the average distance of the 10 closest points to 'p') (Fig 4) and the volume V at end-diastole. The weight is therefore a function of the point density in a defined region, the volume of the heart and the distances between points at end-diastole.

UPV Maximum peak-to-peak voltage (expressed in mV) of the intracardiac signal measured at the tip of the mapping catheter. This unipolar recording may identify subtle changes in the local myocardial voltages.

BPV Maximum peak-to-peak voltage of the cardiac signal measured at the catheter tip and the catheter ring (located more proximally). Although it has been hypothesized that BPV may be more accurate than UPV, because it is less likely to be influenced by contact stability and 'far-field' potentials, only UPV is currently being used in the electromechanical assessment of the left ventricle. Future studies may elucidate the importance of BPV measurements.

The 3-D Mapping Procedure

The mapping catheter is introduced through a 7 or 8Fr femoral sheath. Prior to the actual mapping procedure, heparin is given intravenously (5,000–10,000 IU); additional heparin is given to maintain an activated clotting time (ACT) greater than 200 s. A reference catheter is applied to the back of the patient. the mapping catheter is then inserted into the left ventricle. The location of the tip of the mapping catheter while inside the heart is gated to end diastole and is recorded relative to the fixed reference catheter, thus compensating for subject motion[3].

As the catheter tip is dragged over the left ventricular (LV) endocardial surface, the system continuously analyzes its location in 3-D space without the use of fluoroscopy. The set of points thus collected comprises an irregularly sampled data set of location points that are members of the endocardial surface. Chamber geometry is then recon-

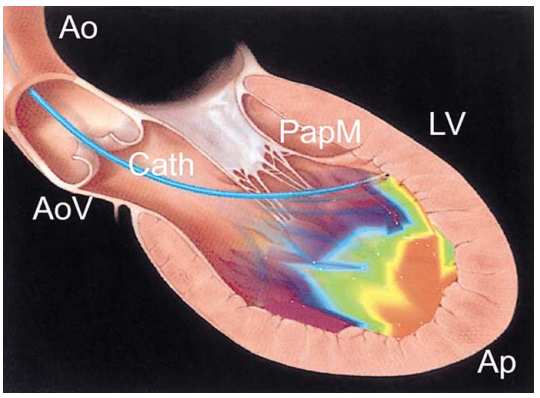

Fig 3. Dragging of the catheter (Cath) through the ventricle with acquisition of electromechanical information. The mapping information is superimposed on the anatomical information. Ao, ascending aorta; AoV, aortic valve; LV, left ventricle; PapM, papillary muscle; Ap, apex of the LV.

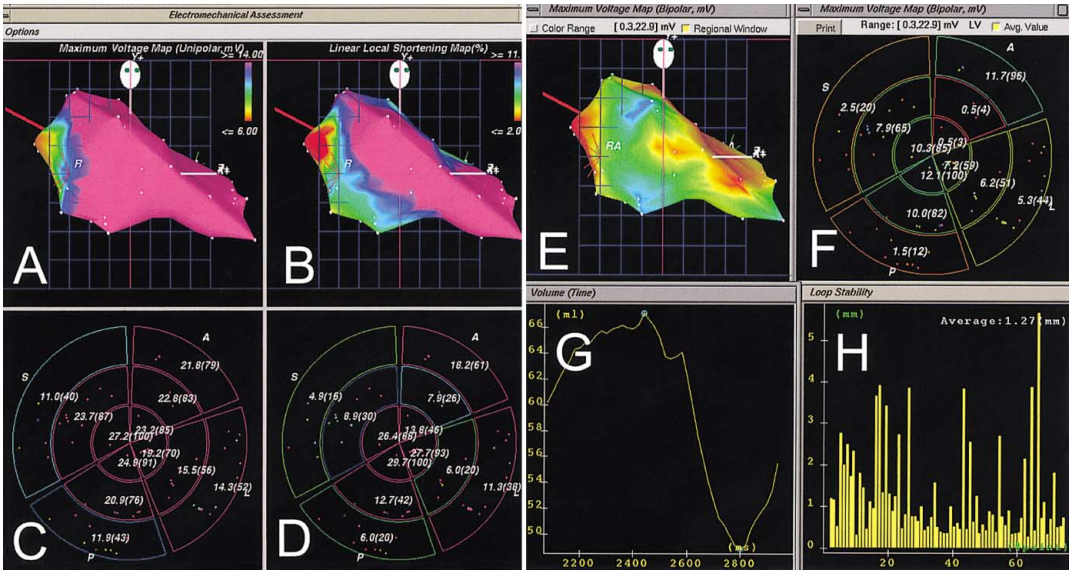

Fig 4. Example of a normal map. (A) Maximum voltage map (unipolar voltage; UPV) in the right anterior oblique (RAO) position. The color bar on the right shows the color coding ranging from red (≤6.0 mV) to blue-purple (≥14.0 mV). (B) The local linear shortening (LLS) map in the same RAO view. The color bar ranges from red (LLS≤2.0%) to blue-purple (≥11.0%). (C) Bull's eye view of the UPV map as displayed by the system. The numbers displayed are the absolute UPV values, with the percentages of the maximum values in parentheses. Four regions (clockwise from top: anterior (A), lateral (L), posterior (P) and septal (S)) are each subdivided into 3 segments (apical, mid and basal), dividing the whole map into 12 segments. (D) Bull's eye view of the LLS map. (E) and (F) show the bipolar map and its bull's eye view, respectively. (G) Volume–time curve, with the blue markers denoting minimum and maximum volumes. (H) Loop stability histograms; the average value of 1.27 mm indicates a reproducible catheter movement trajectory.

structed, in real time, using the set of sampled location points (Fig 3). The endocardial surface is presented as a set of polygons (triangles) whose vertices are the sampled points. The LAT at each site is determined as the time difference between a selected fiducial point on the body-surface ECG and the steepest negative intrinsic deflection in the unipolar intracardiac electrogram (filtered at 0.5–400 Hz) recorded from the tip of the mapping catheter. The activation map is color coded and superimposed on the 3-D chamber geometry. The center of mass of the reconstructed chamber is automatically calculated from the set of the surface points, and the volume of the chamber can be calculated from the sum of the volumes of all tetrahedrons constructed when connecting the center of mass to all triangles forming the reconstructed surface[2] Thus, LV end-diastolic (LVEDV) and end-systolic (LVESV) volumes, stroke volume (SV=LVEDV–LVESV) and ejection fraction (LVEF, SV/LVEDV) can be calculated and displayed (Fig 4).

The stability of the catheter-to-wall contact is evaluated at every site in real time, and points can be manually deleted from the map if one of the following criteria is met: (1) a premature beat or a beat after a premature beat; (2) location stability, defined as a difference of more than 4 mm in the end-diastolic location of the catheter at 2 sequential heartbeats; (3) loop stability, defined as an average distance of more than 4 mm between the location of the catheter at 2 consecutive beats at corresponding time intervals in the cardiac cycle (Fig 4); (4) cycle length that deviated more than 10% from the median cycle length; (5) different morphologies of the local ECG at 2 consecutive beats, or severe ST-elevation of the intracardiac electrogram depicting excessive myocardial impression by the mapping catheter; (6) local activation time differences of more than 3 ms between 2 consecutive beats; (7) different QRS morphologies of the body surface ECG; (8) inner point location; (9) adjacent points closer than 5 mm; or (10) points not related to the left ventricle (such as atrial location)[3] The moderate filtering algorithm incorporated in the system covers most of these issues. A normal map is shown in Fig 4.

Experimental and Clinical Studies

The initial validation studies of the mapping system were reported by Gepstein et al[4] These authors first tested the in vitro accuracy of the locatable-catheter capabilities, using a test jig with several holes at precise known distances from each other, and they showed that repeated measurements of the location of one specific site differed 0.16 mm maximally, and that distances between specific points were equally highly reproducible (mean error, 0.42 mm). Also, the intracardiac electrical signal from the locatable catheter was found to correlate highly with the signal acquired using a standard nonlocatable electrophysiological catheter placed in the immediate vicinity of the mapping catheter (cross-correlation=0.96±0.01). In the same study, they tested the reproducibility of measurements performed in the beating pig's heart. Again, the standard deviation (SD) for measurements at the same site were low (0.74±0.13 mm), and the overall mean error of distances measured inside the body (through the use of a long sheath with markers every 10 mm) proved to be low (0.73±0.03 mm). Furthermore, Gepstein et al found a consistent activation pattern of the left ventricle in pigs. During ventricular pacing, the earliest site of activation was at the site of pacing. During sinus rhythm, the earliest site of activation was on the superior part of the septum. Invariably, the

latest site of activation in both rhythms was on the left lateral wall close to the mitral valve annulus. The total activation time of the left ventricle varied between 40 and 80 ms during sinus rhythm and between 57 and 87 ms during paced rhythm[4].

In a second series of validation studies by the same group, volumetric measurements of test jigs and pig ventricles were analyzed[2]. Phantom objects with known volumes showed that the measured volumes were very close to the actual volumes, with an average deviation of about 2.7%. Measurements of LV casts (with a more difficult anatomy) showed an average deviation of 9.6%, with a correlation r=0.94 with the actual volumes. Measurements of volumes in a dynamic test jig showed high accuracy with known volumes, deviating only 1.4, 0.7, 6.0 and 5.2% for maximal volume, minimal volume, SV and EF, respectively[2]. In 12 pigs tested in this study, the intra- and interobserver variability proved to be very low. Also, SV measurements acquired with the mapping system proved to be highly correlated with thermodilution cardiac output measurements (Fig 7)[2].

As further validation of the system as a tool for the assessment of local LV function, Gepstein et al measured the LV electromechanical regional properties in 11 dogs with chronic infarction (4 weeks after ligation of the proximal left anterior descending coronary artery) and 6 controls and compared them with the pathology results. Average endocardial local shortening (LS, measured at end systole and normalized to end-diastole) and intracardiac bipolar electrogram amplitude were quantified at 13 LV regions. Endocardial LS was significantly lower at the infarcted area (1.2±0.9%, p<0.01) compared with the noninfarcted regions (7.2±1.1–13.5±1.5%) and with the same area in controls (15.5±1.2%, p<0.01). The average bipolar amplitude was also significantly lower at the infarcted zone (2.3±0.2 mV, p<0.01) compared with the same region in the controls (10.3±1.3 mV) and with the noninfarcted regions (4.0±0.7–10.2±1.5 mV, p<0.01) in the infarcted group. Also, the electrical maps could accurately delineate both the location and extent of the infarct, as demonstrated by the high correlation with pathology (Pearson's correlation coefficient = 0.90) and by the precise identification of the infarct border. The authors concluded that chronic infarcted myocardial tissue could be accurately characterized and quantified by its abnormal regional mechanical and electrical functions[5].

The first human studies with the NOGA™ system were reported by Kornowski et al[3] who performed LV endocardial mapping in 24 patients (12 patients with prior myocardial infarction (MI) and 12 control patients) to assess the electromechanical function in infarcted versus healthy myocardial tissue. In patients with prior MI, the average voltage was 7.2±2.7 mV (UPV) / 1.4±0.7 mV (BPV) in the MI region, 17.8±4.6 mV (UPV) / 4.5±1.1 mV (BPV) in healthy zones remote from MI, and 19.7±4.4 mV (UPV) / 5.8±1.0 mV (BPV) in the control patients (p<0.001 for MI values vs remote zones or control patients). They clearly showed that both UPV and local endocardial shortening were significantly impaired in the MI zone compared with controls. Also, concordance with echocardiographic wall motion analysis was good[3]. An example is given in Fig 5.

Kornowski et al later reported on a comparison between NOGA™ mapping and radionuclide perfusion imaging[6]. They showed that UPV (14.0±2.0 mV) and LLS values (12.5±2.8%) were highest when measured in myocardial segments (n=56) with normal perfusion and lowest (7.5±3.4 mV and 3.4±3.4%) when measured in myocardial segments with fixed perfusion defects (n=20) (p<0.0001) on single-photon emission computed tomography imaging studies using ^{201}Tl at rest and ^{99m}Tc-sestamibi after adenosine stress. A significant difference in the UPV and LLS values was found between groups (p<0.001 for each comparison by ANOVA). Myocardial segments with reversible perfusion defects (n=66) had intermediate UPV (12.0±2.8 mV, p=0.048 vs normal and p=0.005 vs fixed segments) and LLS values (10.3±3.7%, p=0.067 vs normal and p=0.001 vs fixed segments). From these results they concluded that NOGA™ mapping might allow the detection of myocardial viability.

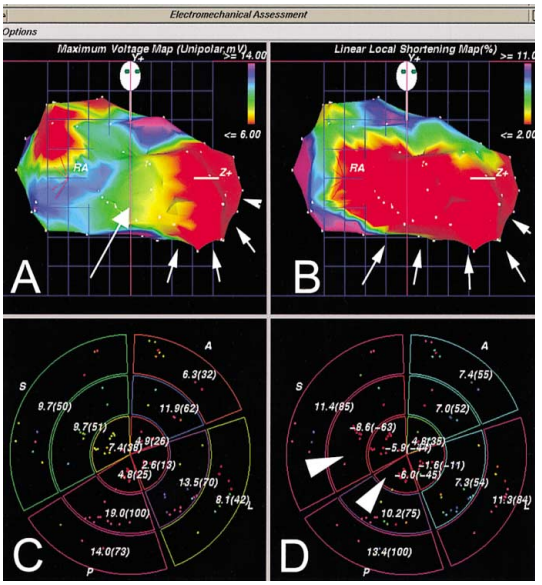

Fig 5. Example of an electromechanical assessment map in a patient with a mid anterior descending artery occlusion and a subsequent apicoposteroseptal infarction. (A) Unipolar voltage (UPV) map and (B) the linear local shortening (LLS) map in the right anterior oblique view. (C) and (D) show the respective bull's eye views. The small arrows in (A) and (B) delineate the infarction zone, which can be clearly appreciated from the red areas. The arrowheads in (D) show the negative LLS values, suggestive of dyskinesia in the apical, septal and posterior regions. The larger arrow in (A) indicates a region of moderate UPV (corresponding with a zone of low LLS), suggestive of viability ('electromechanical mismatch').

Van Langenhove et al compared EDV and ESV, SV and EF in 44 patients using both LV angiography and NOGA™ mapping. Although a strong correlation (r=0.78, p<0.001) for EF measurement between the 2 techniques was found, the Bland–Altman analysis demonstrated the disagreement and absence of interchangeability between the 2 methods. Indeed, on average, a difference of about 30% in LVEF was found[7]. They also compared LLS assessed with nonfluoroscopic electromechanical mapping (NEM) as a function of regional wall motion with echocardiographic data in a subset of 40 patients with severe coronary artery disease and subsequently decreased LV function. That study showed that NEM mapping can accurately assess regional wall motion, and also showed a significant decrease in UPV in segments with declining regional function[8]. The same authors described significant correlations between regional wall motion assessment using LV angiography as compared with LLS data acquired in the same segments (p<0.001) (see Fig 6)[9]. Finally, Van Langenhove's group compared

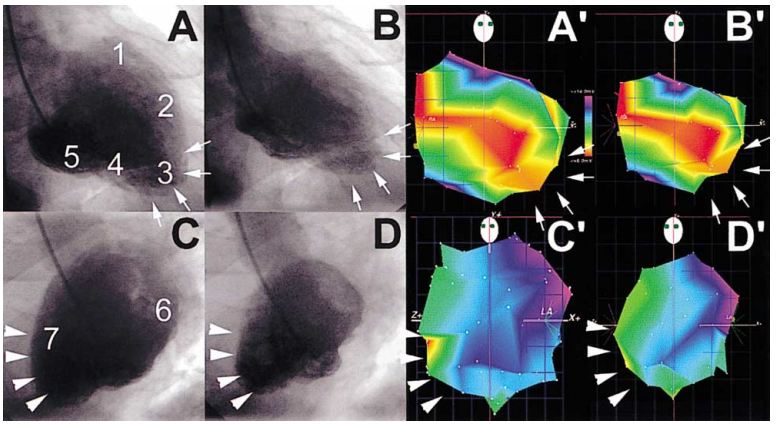

Fig 6. Left ventricular angiogram in right anterior oblique view (A,B) and left anterior oblique view (C,D) views in, respectively, end-diastole (A,C) and end-systole (B,D). Corresponding linear local shortening (LLS) map in the same views (A'–D'). The arrows in (A,B) indicate areas suggestive of apical akinesia, the arrowheads in (C,D) show akinesia in the septal region. The arrows in (A',B') show the red zone in the apical region; low LLS values are also found in the septal region (arrowheads; red zone in septal area in A',B' and red-yellow-green zone in C',D').

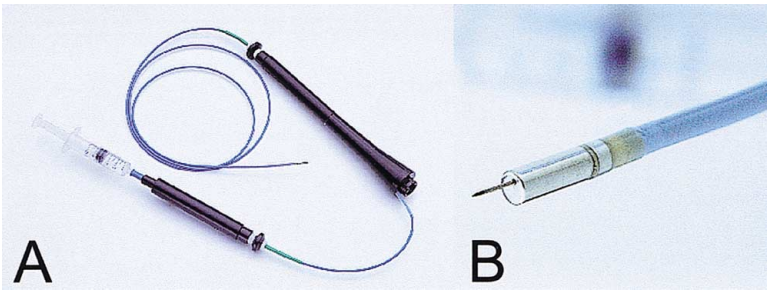

Fig 7. The Biosense injection catheter (A) and catheter tip (B). The catheter has a 7Fr shaft with a distal active deflectable tip of 8Fr. The tip consists of an electromagnetic sensor, a ring and tip electrode and the housing of a 0.014×0.009 inch extendable nitinol needle (B). At the proximal end of the catheter, the nitinol shaft has a Luer lock fitting for a syringe, which may contain injectable substances.

dobutamine stress echo with the LLS and UPV data for comparable segments in patients with a previous MI. The ROC curves showed significant cut-off values for myocardial viability of UPV = 9.0 mV (sens 56%, spec 81%, p< 0.0001) and LLS = 6.8% (sens 56%, spec 92%, p<0.0001) (see also Fig 5).[10,11]

Fuchs et al used the NOGA™ to assess the in-vivo electromechanical changes following gradual coronary artery occlusion in a pig ameroid constrictor model.[12] UPV and LLS were measured in the ischemic lateral and non-ischemic anterior zones in animals at rest (n=9) and at 5 weeks after the implantation of ameroid constrictors around the left circumflex artery. Echocardiography was used to assess regional contractility (% myocardial thickening), and an echo-contrast perfusion study was performed using acoustic densitometry methods. The ischemic lateral zone showed reduced myocardial perfusion at rest (peak intensity; 3.4±1.7 vs 20.7±14.8, p=0.005), impaired mechanical function (% wall thickening 22±19% vs 40±11%, p=0.03; local endocardial shortening 2.9±5.5% vs 11.7±2.1%, p= 0.002), and preserved electrical activity (UPV 12.4±4.7 vs 14.4±1.9 mV, p=0.25; BPV 4.1±1.1 vs 3.8±1.5 mV, p=0.62) compared with the anterior region. The authors concluded that gradual coronary artery occlusion resulting in regional reduced perfusion and function at rest (ie, hibernating myocardium) is characterized by preserved electrical activity, so electromechanical LV mapping may be of diagnostic value for identifying this type of myocardial injury.[12] Botker et al compared the findings of fluorodeoxyglucose-positron emission tomography with data derived from NOGA™ mapping and found that segments with reversible perfusion defects had UPV/LLS of 7.3±3.1 mV and 4.0± 2.4%, respectively. Normal segments showed UPV 11.5±3.7 mV and LLS 7.7±3.3%. Infarcted areas with irreversible perfusion defects showed UPV 4.8±2.2 mV and LLS 2.9± 2.8%.[13]

Kornowski et al recently presented preliminary results on the first NOGA™-guided direct myocardial revascularization (DMR) study.[14] DMR using this technique was safe and feasible, in so far as no deaths occurred in the 77 patients, and early efficacy endpoints showed an improvement in anginal status and prolonged exercise capacity 6 months after the index procedure. Laham et al reported on improvement in regional wall motion score and collateralization in a subgroup of 15 patients also treated with laser-DMR.[15] Some caution, however, may be appropriate. As previous studies have reported that a substantial number of patients suffer an episode of heart failure following transmyocardial laser revascularization,[16,17] we sought to determine the acute effects on LV function. We found that in 15 patients, in whom we performed a LV angiogram before and immediately after the DMR procedure, the relative decrease in LVEF was 18%±10 after DMR, and the relative decrease in regional wall motion was 9%±18 for the non-treated and 26%±17 for the treated regions. From this study, we concluded that the physician should be cautious when performing myocardial laser revascularization in patients with a low (<30%) baseline LVEF.[18]

Recently, Vale et al showed the feasibility and safety of percutaneous, catheter-based, nonfluoroscopic mapping guided myocardial gene-transfer.[19] In 6 pigs in which the injection catheter was used to deliver plasmid using cytomegalovirus promoter/enhancer, encoding nuclear-specific LacZ (pCMV-nlsLacZ) (50 μg/ml) to a single LV myocardial region, peak β-galactosidase activity after 5 days was documented in the target area in each pig. All pigs survived until they were killed, and no complications were observed with either the mapping or injection procedures, so the authors concluded that percutaneous myocardial gene-transfer can be successfully achieved in normal and ischemic

myocardium without significant morbidity or mortality![19] It is furthermore important to underline the importance of the 3-D mapping technique for gene application procedures, as exact delineation of the area to be treated is mandatory. To test the feasibility of myocardial angiogenic gene expression, through endocardial transfection of adenovirus vascular endothelial growth factor-121, using the NOGA™ system for guidance, Kornowski et al transfected transgenes into designated myocardial sites of the pig model. They demonstrated that this less invasive catheter-based system offers a similar gene delivery efficiency and thus may have clear advantages over the surgically-based transepicardial injection approach![20] In a recent study, Smits et al demonstrated in a pig model that the average efficiency of an endomyocardial catheter injection using the NOGA™ system for guidance is 26±23%, and that intramyocardial retention after endomyocardial injection of small proteins, such as albumin, is short compared with the stable retention rates of small particles such as colloid–albumin![21] An injection catheter is shown in Fig 7.

Ongoing and Clinical Investigations

Some burning questions related to the clinical application of the NOGA™ mapping system in clinical practice still need to be addressed. Up to now, there has not been clear evidence that the local shortening function really is a reflection of local wall motion. We do not know if assessment of BPV could further improve the performance of the system nor do we know if the system is able to detect true viability. It also needs to be further investigated whether there is a requirement for this expensive technique for in-cathlab detection of viability/ischemia, when other techniques have already proven their value, and whether direct myocardial revascularization, for which this system seems to be the ideal guiding tool, really improves the clinical status of the patient. It is also unclear if local gene application, again for which this system seems an optimal platform, will be applied clinically.

Some of these questions will be answered by ongoing investigations. The DIRECT trial in the USA (a single blinded, randomized NOGA™ mapping with and without DMR in patients not suitable for classical revascularization) is aiming to answer the question of whether the presumed benefit with DMR is simply a placebo effect, or does it really improve the patient's clinical and functional status. The DIRECT trial has included 300 patients and the first results have been presented at recent international conferences. Although not yet published, DMR did not seem to have any beneficial effect on true ischemia, but did seem to benefit patients (on average, a 2-level reduction in ischemia class). Published data, however, need to be available to further evaluate the possible future use of this therapeutic approach. Studies assessing 'true viability' in patients scheduled for bypass surgery will answer the question of whether NOGA™ can predict the recuperation after revascularization of myocardial segments with wall motion abnormalities. The DINO study is currently enrolling patients and the goal of this trial is to assess the possibilities of the NOGA™ system to accurately determine viability in hibernating myocardial segments, as compared with stress echocardiography, radionuclide perfusion scintigraphy and angiography performed before and 6 months after coronary bypass surgery. A study assessing the possible additional benefit of low-dose dobutamine during NOGA™ mapping is currently being performed at the Thoraxcenter. Future investigations will evaluate the possible value of adenosine in the detection of ischemic segments, the diagnostic value of NOGA™ mapping as compared with MRI in myocardial viability, the efficacy of growth factors to induce myocardial angiogenesis and additional comparisons with radionuclide perfusion imaging studies![13–15,22,23] In addition, Kornowski et al currently investigating the possibility of a pericardial approach to acquire electromechanical mapping information and whether intrapericardial delivery of angiogenic factors may offer a theoretical advantage over prolonged exposure of either coronary or myocardial tissue to the administered drug as result of the reservoir function of the pericardium![24]

Investigations to shorten the mapping time, to acquire multiple point information through a multi-sensor catheter, and to incorporate fluoroscopic information into the NOGA™ system are underway.

Conclusions

Left endoventricular 3-D real-time electromechanical mapping is a new, intriguing technique for in-cathlab assessment of the mechanical and electrical functioning of the left ventricle. Although initial studies have shown the safety, feasibility and reproducibility of this technique, and have provided similar results when compared with established techniques used to investigate myocardial viability, data on the additional clinical value of the system are still scarce. Ongoing trials on the prediction of viability, the benefit of DMR and intramyocardial gene injection may definitely establish its place among currently used techniques in interventional cardiology.

References

1. Ben-Haim SA, Osadchy D, Schuster I, Gepstein L, Hayam G, Josephson ME: Nonfluoroscopic, *in vivo* navigation and mapping technology. *Nat Med* 1996; **2:** 1393–1395
2. Gepstein L, Hayam G, Shpun S, Ben-Haim SA: Hemodynamic evaluation of the heart with a nonfluoroscopic electromechanical mapping technique. *Circulation* 1997; **96:** 3672–3680
3. Kornowski R, Hong MK, Gepstein L, Goldstein S, Ellahham S, Ben-Haim SA, et al: Preliminary animal and clinical experiences using an electromechanical endocardial mapping procedure to distinguish infarcted from healthy myocardium. *Circulation* 1998; **98:** 1116–1124
4. Gepstein L, Hayam G, Ben-Haim SA: A novel method for nonfluoroscopic catheter-based electroanatomical mapping of the heart. In vitro and *in vivo* accuracy results. *Circulation* 1997; **95:** 1611–1622
5. Gepstein L, Goldin A, Lessick J, Hayam G, Shpun S, Schwartz Y, et al: Electromechanical characterization of chronic myocardial infarction in the canine coronary occlusion model. *Circulation* 1998; **98:** 2055–2064
6. Kornowski R, Hong MK, Leon MB: Comparison between left ventricular electromechanical mapping and radionuclide perfusion imaging for detection of myocardial viability. *Circulation* 1998; **98:** 1837–1841
7. Van Langenhove G, Hamburger J, Smits P, et al: Nonfluoroscopic electromechanical mapping for evaluation of left ventricular hemodynamics: A comparison with contrast ventriculography. *Acta Cardiol* 1999 (in press)
8. Van Langenhove G, Hamburger J, Albertal M, Smits P, Onderwater E, Serruys P: Comparison of mechanical properties of the left ventricle in patients with severe coronary artery disease by nonfluoroscopic mapping versus two dimensional echocardiograms. *Am J Cardiol* 2000 (in press)
9. Van Langenhove G, Smits P, Serrano P, et al: Assessment of regional wall motion: A comparison between computerized LV angiography and nonfluoroscopic electromechanical mapping (abstract). *Circulation* 1999; **100:** I-725
10. Van Langenhove G, Smits P, Albertal M, et al: NOGA mapping for

the detection of viable and ischemic myocardium: A comparison with dobutamine stress echocardiography (abstract). *Circulation* 1999; **100:** I-23
11. Van Langenhove G, Smits P, Hamburger J, Serrano P, Serruys P: Hibernating myocardium diagnosed with nonfluoroscopic electromechanical (NOGA) mapping: A comparison with dobutamine stress echocardiography. *J Am Coll Cardiol* 2000; **35:** 81A
12. Fuchs S, Kornowski R, Shiran A, Pierre A, Ellahham S, Leon MB: Electromechanical characterization of myocardial hibernation in a pig model. *Coron Artery Dis* 1999; **10:** 195–198
13. Botker H, Lassen J, Bottcher M, et al: Left ventricular electromechanical mapping for detection of myocardial viabilityin patients with impaired left ventricular function due to chronic ischemic heart disease (abstract). *Circulation* 1999; **100:** I-22
14. Kornowski R, Baim D, Moses J, et al: Six month results following percutaneous direct myocardial revascularization guided by Biosense left ventricular mapping in patients with refractory coronary ischemic syndromes (abstract). *Circulation* 1999; **100:** I-22
15. Laham R, Pearlman J, Datta R, Gao L, Baim D: Biosense-guided laser myocardial revascularization improves 30-day and 6-month regional wall motion, perfusion and collateralization of the treated zone (s) (abstract). *Circulation* 1999; **100:** I-22
16. Frazier OH, March RJ, Horvath KA: Transmyocardial revascularization with a carbon dioxide laser in patients with end-stage coronary artery disease [see Comments]. *N Engl J Med* 1999; **341:** 1021–1028
17. Allen KB, Dowling RD, Fudge TL, Schoettle GP, Selinger SL, Gangahar DM, et al: Comparison of transmyocardial revascularization with medical therapy in patients with refractory angina [see Comments]. *N Engl J Med* 1999; **341:** 1029–1036
18. Van Langenhove G, Regar E, Foley DP, Hamburger JN, Smits PC, Albertal M, et al: Acute changes of global and regional left ventricular function immediately after direct myocardial revascularization. *Semin Intervent Cardiol* 2000; **5:** 103–106
19. Vale PR, Losordo DW, Tkebuchava T, Chen D, Milliken CE, Isner JM: Catheter-based myocardial gene transfer utilizing nonfluoroscopic electromechanical left ventricular mapping. *J Am Coll Cardiol* 1999; **34:** 246–254
20. Kornowski R, Leon MB, Fuchs S, Vodovotz Y, Flynn MA, Gordon DA, et al: Electromagnetic guidance for catheter-based transendocardial injection: A platform for intramyocardial angiogenesis therapy: Results in normal and ischemic porcine models. *J Am Coll Cardiol* 2000; **35:** 1031–1039
21. Smits P, Van Langenhove G, Schaar M, et al: Efficiency of percutaneous intramyocardial injections using a nonfluoroscopic 3-D mapping based catheter system. *Cardiovasc Res* 2000; (in press)
22. Vale P, Tkebuchava T, Milliken C, Chen D, Symes J, Isner J: Percutaneous electromechanical mapping demonstrates efficacy of pVGI.1 (VEGF2) in an animal model of chronic myocardial ischemia (abstract). *Circulation* 1999; **100:** I-22
23. Fuchs S, Hendel R, Kuntz R, et al: Left ventricular electromechanical mapping reflects resting myocardial perfusion and viability: Comparative analysis with SPECT radionuclide myocardial imaging (abstract). *Circulation* 1999; **100:** I-22
24. Kornowski R, Fuchs S, Leon MB, Epstein SE: Delivery strategies to achieve therapeutic myocardial angiogenesis. *Circulation* 2000; **101:** 454–458